



**VICTORIA UNIVERSITY**  
MELBOURNE AUSTRALIA

*Effects of Landscape Design on Urban Microclimate  
and Thermal Comfort in Tropical Climate*

This is the Published version of the following publication

Yang, Wei, Lin, Y and Li, CQ (2018) Effects of Landscape Design on Urban Microclimate and Thermal Comfort in Tropical Climate. *Advances in Meteorology*, 2018. ISSN 1687-9309

The publisher's official version can be found at  
<https://www.hindawi.com/journals/amete/2018/2809649/>  
Note that access to this version may require subscription.

Downloaded from VU Research Repository <https://vuir.vu.edu.au/37777/>

## Research Article

# Effects of Landscape Design on Urban Microclimate and Thermal Comfort in Tropical Climate

Wei Yang,<sup>1,2</sup> Yaolin Lin <sup>1</sup> and Chun-Qing Li <sup>3</sup>

<sup>1</sup>School of Civil Engineering and Architecture, Wuhan University of Technology, Wuhan 430070, China

<sup>2</sup>College of Engineering and Science, Victoria University, Melbourne, VIC 8001, Australia

<sup>3</sup>School of Engineering, RMIT University, Melbourne, VIC 3000, Australia

Correspondence should be addressed to Yaolin Lin; yaolinlin@gmail.com

Received 11 May 2018; Revised 17 July 2018; Accepted 31 July 2018; Published 29 August 2018

Academic Editor: Andreas Matzarakis

Copyright © 2018 Wei Yang et al. This is an open access article distributed under the Creative Commons Attribution License, which permits unrestricted use, distribution, and reproduction in any medium, provided the original work is properly cited.

A climate-responsive landscape design can create a more livable urban microclimate with adequate human comfortability. This paper aims to quantitatively investigate the effects of landscape design elements of pavement materials, greenery, and water bodies on urban microclimate and thermal comfort in a high-rise residential area in the tropic climate of Singapore. A comprehensive field measurement is undertaken to obtain real data on microclimate parameters for calibration of the microclimate-modeling software ENVI-met 4.0. With the calibrated ENVI-met, seven urban landscape scenarios are simulated and their effects on thermal comfort as measured by physiologically equivalent temperature (PET) are evaluated. It is found that the maximum improvement of PET reduction with suggested landscape designs is about 12°C, and high-albedo pavement materials and water bodies are not effective in reducing heat stress in hot and humid climate conditions. The combination of shade trees over grass is the most effective landscape strategy for cooling the microclimate. The findings from the paper can equip urban designers with knowledge and techniques to mitigate urban heat stress.

## 1. Introduction

The world is at its fastest pace of urbanization. Since 2008, more than half of the world's population live in urban areas. The trend in global population increase has led to an increase in housing demand. Singapore has gone from one of the worst housing shortages in the world in the 1960s to a country where 90% of its citizens now own their own home and homelessness is virtually eliminated—despite its population has tripled in the last 50 years. With success of housing policies, natural land has been replaced by artificial surfaces in Singapore with undesirable thermal effects. This issue, together with increasing industrialization, has caused a considerable deterioration of the urban environment. In tropical countries like Singapore, hot climate in terms of high temperature, high humidity, and high solar radiation often causes heat stress to residents, resulting in negative impact on public health and productivity. Climate-responsive urban design can create microclimates that people experience as feeling cooler than the prevailing climate, making urban spaces pleasant.

Thus, the effect of urban landscaping on microclimate and human thermal comfort is necessary to be considered in the urban design and planning process.

It is acknowledged that the transfer of climatic knowledge into planning practice is still lacking [1, 2]. Although many measures to reduce urban heat stress and/or improve outdoor thermal comfort have been proposed by various researchers and at different spatial scales [2–6], their effectiveness is a subject for debate. The main reason is that the dominant professions for urban design and planning, namely, architecture and engineering, so far focus on the influence of landscaping on air and surface temperatures and their subsequent effect on buildings [7]. However, the impact of countermeasures by urban design on urban thermal comfort cannot be described sufficiently by simple microclimate factors, such as surface or air temperature. There are seven factors (or parameters) that affect human thermal comfort in an outdoor environment. They are air temperature, air humidity, wind, solar radiation, terrestrial radiation, metabolic heat, and clothing insulation [8]. The first

five parameters are affected by urban environments, while the latter two are related to individual choice. At the neighborhood or community scale, landscape elements can modify not only the wind and radiation but also the air temperature and humidity [2–9]. Therefore, it is necessary to study the effect of different landscape elements on different microclimate parameters and corresponding human thermal comfort.

In recent years, some researchers have realized that urban heat stress can be reduced through appropriate landscape design. Many field measurements and numerical simulations have been carried out to study the effect of landscape elements on urban microclimate and thermal comfort. For example, Ng et al. [5] conducted parametric studies in Hong Kong and found that proper greening may greatly improve the urban microclimate and lower the summer urban air temperature. Yahia and Johansson [10] explored how vegetation and landscape elements affect outdoor thermal comfort for detached buildings in the hot dry climate of Damascus, Syria, and found that PET (physiologically equivalent temperature) can be reduced by about 19°C for east-west street orientation through appropriate landscape design. Perini and Magliocco [11] investigated effects of vegetation, urban density, building height, and atmospheric conditions on local temperatures and thermal comfort in three different cities in Italy and found that vegetation has higher cooling effects with taller buildings. Lee et al. [12] studied the potential of urban green coverage to mitigate human heat stress using the ENVI-met model and found that trees are more effective in mitigating human heat stress than just grasslands. Yahia et al. [2] investigated the relationship between urban design, urban microclimate, and outdoor comfort in four built-up areas with different morphologies and found that the use of dense trees helps to reduce heat stress, but vegetation might negatively affect the wind ventilation.

Although the previous studies have added new knowledge and provided new insights, they have mainly focused on the street design like street orientation, street greenery, and street geometry [3–5, 10, 13]. Little research has been conducted in urban residential areas, particularly in those with high-rise residential areas. The microclimate quality of outdoor spaces in a residential area affects the quality of life of its residents. Therefore, the aim of this paper is to investigate how landscape elements affect urban microclimate and human thermal comfort in a high-rise residential area in Singapore by investigating different landscape design scenarios of pavement materials, greenery, and water bodies. Studying the relationship between landscaping and microclimate in cities like Singapore can provide valuable guidance, both for keeping Singapore residents cool and informing temperate-climate cities that would be much warmer in the future.

## 2. Materials and Methods

**2.1. Study Area.** The study area is two residential quarters at Bedok in southeast Singapore as shown in Figure 1. Bedok is an urban residential zone for new development in Singapore. The two residential quarters are condominiums named the Clearwater and Aquarius By The Park near Bedok Reservoir.



FIGURE 1: Study area and field measurement points at Bedok.

The two residential quarters are in close proximity to each other with the Clearwater on the west side of Bedok Reservoir View Road and Aquarius By The Park on the east side of the road. Buildings in the studied residential quarters are of 4 to 18 storeys. An urban park is located in the vicinity of the two residential quarters on the north.

**2.2. Field Measurements.** Field measurements were conducted at the study area from 13 April to 06 June 2012. The purpose of field measurements is to validate ENVI-met modeling (see below) results and also help define the initial conditions of the general model of ENVI-met.

Five measurement points were stationed as shown in Figure 1. The measurement points were selected to represent variations in urban geometry, ground thermal properties, and greenery as shown in Figure 2. Points 1 and 2 are in the urban park, and points 3, 4, and 5 are in a high-density apartment area. The sky view factor (SVF) ranges from highly shaded point 2 (SVF = 0.17) to less shaded point 5 (SVF = 0.67). The measured microclimatic parameters are air temperature, globe temperature, relative humidity, and wind speed, which were measured for 24 hours continuously and taken at 2.0 m above the ground level. Table 1 shows the measured microclimatic parameters and equipment used for the field measurements.

**2.3. Microclimate Simulation.** For this study, the thermal characteristics of different urban design scenarios were investigated by ENVI-met 4.0 [14, 15]. This is a microclimate analysis program that simulates the thermal characteristics and energy fluxes in the built environment with high spatial and temporal resolution. The model generates a large amount of output data including necessary variables for calculation of thermal stress indices. It has been employed by many researchers to study the effects of different urban design options on microclimate and outdoor thermal comfort [1–4, 10–13]. ENVI-met 4.0 allows users to employ the measured meteorological data as inputs by forcing the model to follow user's inputs during the simulation. In the previous versions of ENVI-met, only relatively simple weather profiles as prescribed by ENVI-met can be used as

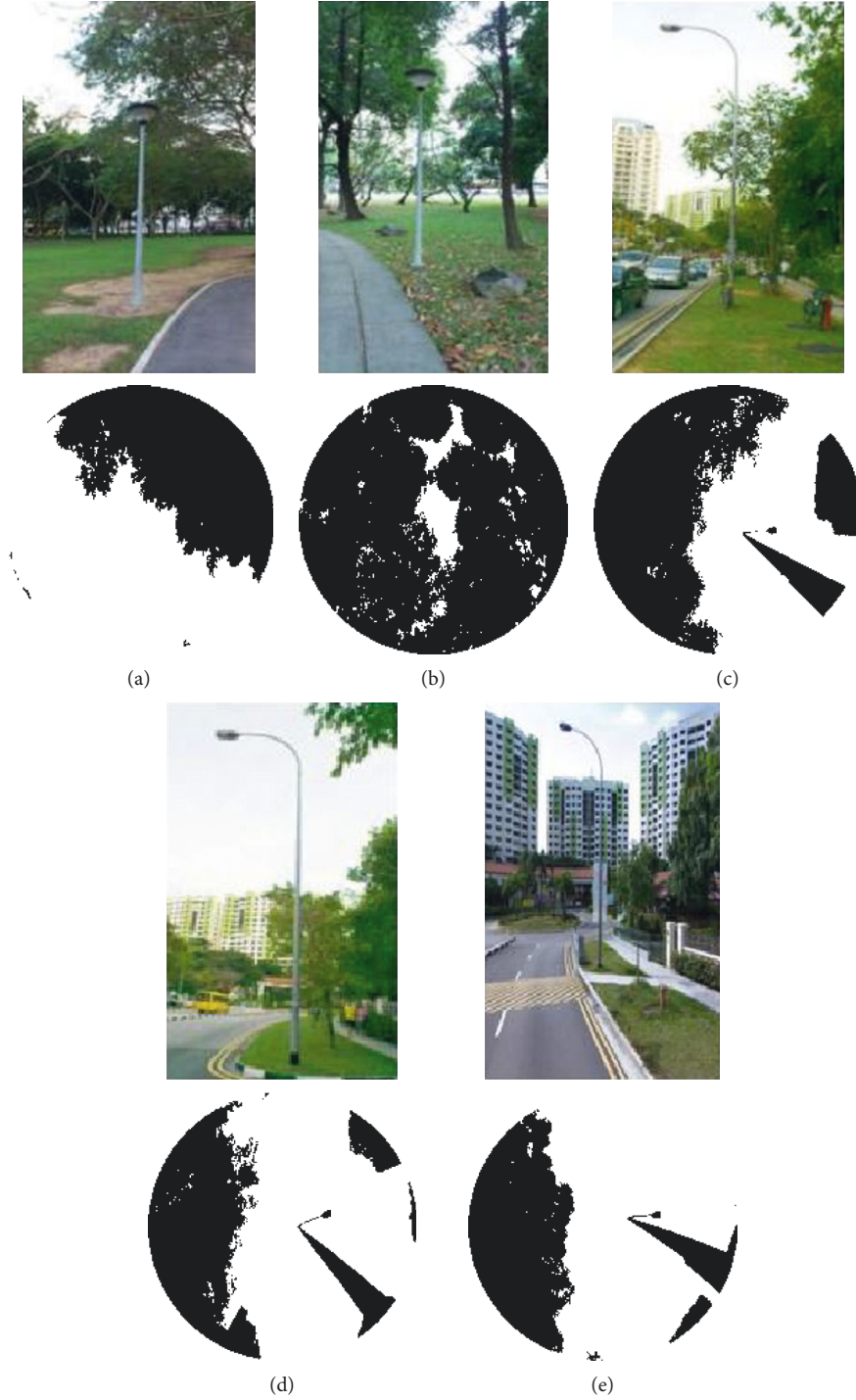


FIGURE 2: Photos and fisheye photos for each location (measurements were taken at 2.0 m above the ground level). (a) Point 1 (SVF = 0.61). (b) Point 2 (SVF = 0.17). (c) Point 3 (SVF = 0.48). (d) Point 4 (SVF = 0.66). (e) Point 5 (SVF = 0.67).

inputs. The details of the ENVI-met model have been fully explained and presented on its website [15] and in many research papers [1, 4, 14, 16].

The weather data from the nearest station at the Changyi Airport were selected. It was found that the daily air temperature on April 30, 2012, was the highest during the study period. Therefore, the simulation study was conducted on that day. The hourly meteorological data from the weather

station and from the on-site observation were used to generate the “forcing file” (as inputs) for the simulation. It was observed that the weather condition during the measurement period was characterized by high temperature, strong solar radiation, and light wind with a prevailing wind direction of southwest. The model was run for 18 h starting at 4 am and ending at 10 pm for each simulation of microclimate.



TABLE 1: Equipment used for field measurement.

Variable	Instrument	Accuracy
Air temperature/ relative humidity	HOBO U12-012 Temp/RH Data Logger	$\pm 0.35^{\circ}\text{C}$ from $0^{\circ}\text{C}$ – $50^{\circ}\text{C}$ to a maximum of $\pm 3.5\%$
Globe temperature	HOBO Thermocouple Data Logger, U12-014 with Type-T Copper-Constantan thermocouple sensors and 40 mm diameter ping pong ball	$\pm 1.5^{\circ}\text{C}$
Wind speed	Onset Wind Speed Smart Sensor, S-WSA-M003	$\pm 1.1\text{ m/s}$ or $\pm 4\%$ of reading, whichever is greater
Short- and long-wave radiation	Kipp & Zonen, CNR 4 with integrated pyranometer, pyrgeometer, Pt-100, and thermistor	Pyranometer: $<5\%$ uncertainty (95% confidence level) Pyrgeometer: $<10\%$ uncertainty (95% confidence level) Pt-100/thermistor: $\pm 0.7^{\circ}\text{C}$

**2.4. Parametric Study and Urban Thermal Comfort Assessment.** The parametric study consists of a base case and seven design scenarios. The base case was constructed according to the actual conditions of the study area. The model domain covers the entire area of the study area and is expanded to the surrounding buildings, streets, and an urban park. The spatial extent of the study area is  $600 \times 392 \times 120\text{ m}$  in the X, Y, and Z dimensions, respectively. The horizontal and vertical grid resolutions are both set at 4 m. The model domain of the base case for the study area is shown in Figure 3. The input data of the general model setting, the initial atmospheric/soil condition, and the building properties are summarized in Table 2.

The other scenarios to be investigated are designed based on changing different landscape elements such as pavement materials (brick, concrete, wood, and light-color granite) and amount of trees, grass, and water bodies as listed in Table 3. For the first 5 scenarios, only one parameter is changed at a time in order to determine the relative effect of each. The last two scenarios are a combination of two design elements to further investigate the effect of ground materials and tree shading.

For the assessment of urban thermal comfort, the PET (physiologically equivalent temperature) is selected as the thermal comfort index. PET has been calibrated against subjective thermal sensation evaluation by Yang et al. [17] in Singapore (Table 4), which makes it possible to compare different urban design proposals. Tropical residents are found to tolerate higher levels of PET than Western/Middle European residents due to thermal adaption to the local climate. PET is calculated using the RayMan model [18, 19]. It can be easily estimated with air temperature, relative humidity, wind speed, mean radiant temperature, clothing, and activity level of people. The thermal comfort map in terms of PET is generated in the paper for comparison.

### 3. Results and Discussion

**3.1. The Base Case Scenario: Measurement and Simulation.** The microclimatic parameters of air temperature, mean radiant temperature, wind speed, and relative humidity collected at measuring points 1–5 have been compared with the corresponding ENVI-met model outputs.

Figure 4 shows the comparison between measured and simulated air temperatures. It can be seen that the simulated and measured air temperatures have the same



FIGURE 3: Model domain for the study area.

TABLE 2: Boundary conditions and initial setting of the ENVI-met model.

Location	Singapore $103^{\circ}51'\text{E}$ , $1^{\circ}18'\text{N}$
Climate	Tropical climate
Date/time simulated	From 04:00 to 22:00 (18 h) on 30 April 2012
Model domain	Bedok: $150 \times 98 \times 30$ grids $\Delta x = \Delta y = \Delta z = 4\text{ m}$ Note: vertical grid with the equidistant method
Meteorological inputs	Air temperature and relative humidity: hourly data from the measurement on-site Wind speed and direction: hourly data from the meteorological station
Initial soil temperature and relative humidity	Specific humidity (2500 m) = $7\text{ g/kg}$ Upper layer (0–20 cm): $305\text{ K}/30\%$ Middle layer (20–50 cm): $307\text{ K}/40\%$ Deeper layer (below 50 cm): $306\text{ K}/50\%$ Inside temperature = $293\text{ K}$ (constant)
Building conditions	Heat transmission walls = $1.94\text{ W/m}^2\cdot\text{K}$ Heat transmission roofs = $6\text{ W/m}^2\cdot\text{K}$ Albedo walls = 0.2 Albedo roofs = 0.3
Plants	Trees: 10 m dense, leafless base Trees: 20 m dense, leafless base Grass: 20 cm average dense

trend for all five points with perhaps more smooth curves for the simulated ones. The air temperature pattern is clearly influenced by the sky view factor and surrounding urban environment. Point 2 has the lowest air temperature

TABLE 3: Different design scenarios for Bedok.

Design scenario	Pavement materials	Vegetation and water body
Base case	Red brick (ID: KK) and concrete pavement (ID: PP)	Sparse trees and grass Small area of water bodies (30 m <sup>2</sup> )
Scenario 1	Wooden boards (ID: WD)	As base case
Scenario 2	Light-color granite (ID: G2)	As base case
Scenario 3	Grass surface	As base case
Scenario 4	As base case	Add more trees (increase by 200%)
Scenario 5	As base case	Add more water bodies (increase by 200%)
Scenario 6	Light-color granite (ID: G2)	Add more trees (increase by 200%)
Scenario 7	Grass surface	Add more trees (increase by 200%)

TABLE 4: Thermal sensations and PET classes for Singapore and Western/Middle Europe.

Thermal sensation	PET range for Singapore (°C)	PET range for Western/Middle Europe (°C)
Very cold	Not applicable	<4
Cold	Not applicable	4–8
Cool	Not applicable	8–13
Slightly cool	20–24	13–18
Neutral	24–30	18–23
Slightly warm	30–34	23–29
Warm	34–38	29–35
Hot	38–42	35–41
Very hot	>42	>41

Source: Yang et al. [17].

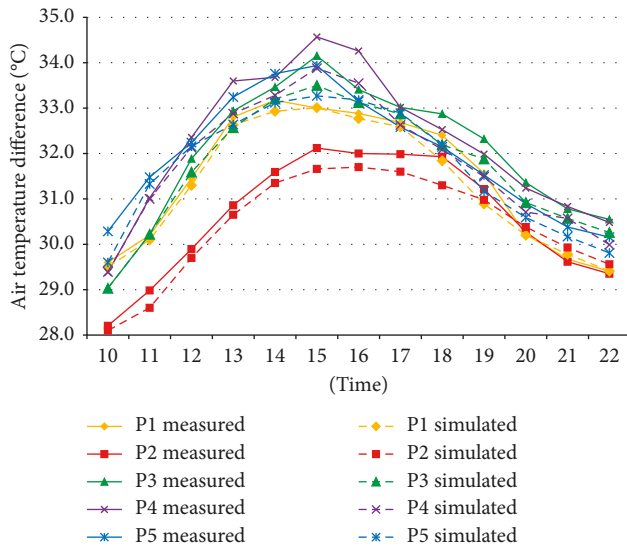


FIGURE 4: Comparison between simulated and measured air temperatures.

because it is located in the nearby park and has a low sky view factor (0.17).

Points 3, 4, and 5 have higher air temperatures than points 1 and 2 because these three points are located along high-density residential buildings. It can also be seen that ENVI-met underestimates the daytime air temperature by about 0.1–0.7°C. This is because ENVI-met calculates the urban climate at a microscale or a local scale and that larger regional

(mesoscale) effects are not taken into account [15]. During the night, the air temperature is underestimated by up to 0.5°C and overestimated by up to 0.3°C with ENVI-met in this study.

The mean radiant temperature comparison between simulated and measured results is shown in Figure 5. It can be seen that the simulated and measured mean radiant temperatures have the same trend for all the points. Points 3, 4, and 5 have a higher mean radiant temperature profile than points 1 and 2 during the day. This is because points 1 and 2 are located in the park and have lower sky view factors. It can also be found that the daytime mean radiant temperature is overestimated and nighttime mean radiant temperature is underestimated by ENVI-met. The daytime difference is about 0.1–6.7°C, and the nighttime difference is about 2.6–6.6°C. A number of other studies have also reported a mean radiant temperature difference of up to 7.97°C between the measured and simulated results [1, 4, 13, 20]. The discrepancies are due to that ENVI-met does not consider heat storage and transfer by buildings or anthropogenic heat production in an adequate manner [13, 21]. Therefore, studies on the effect of landscape design on nighttime outdoor thermal comfort and urban heat island need further investigation in the future due to limitations of ENVI-met modeling.

The results of the measured and simulated wind speed and relative humidity show little difference (less than 5%) for all the points. The input wind speed is less than 2 m/s in this study. It has also been reported that wind speeds predicted by ENVI-met are consistent with field data for input wind speeds below 2 m/s [22].

Tables 5 and 6 show the model fit between simulated and measured results for air temperature and mean radiant temperature, respectively. Very high overall agreement can be found for both air temperature ( $R^2$  between 0.95 and 0.99) and mean radiant temperature ( $R^2$  between 0.74 and 0.96). The relatively lower model fit of  $R^2 = 0.74$  for point 2 as well as the 5°C difference between simulated and measured results in terms of mean radiant temperature can be partially explained by the error in the measurement; for example, solar radiation suddenly became very intense during that particular measurement time.

Therefore it is possible to say that although there are some discrepancies between the simulated and measured results, ENVI-met is able to present similar trends for microclimatic parameters compared with those from field measurement. Compared with a former study conducted in

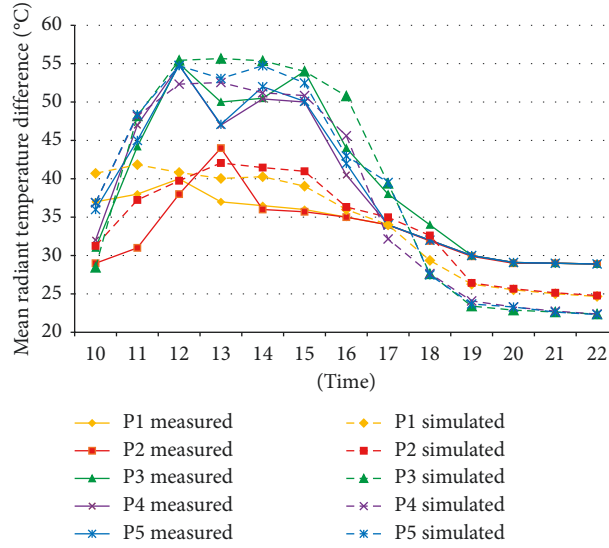


FIGURE 5: Comparison between simulated and measured mean radiant temperatures.

TABLE 5: Model fit between simulated and measured results for air temperature.

	Point 1	Point 2	Point 3	Point 4	Point 5
Minimum error (°C)	0	-0.1	0	0.01	0.03
Maximum error (°C)	-0.67	-0.63	-0.68	-0.72	-0.67
Mean error (°C)	-0.16	-0.19	-0.31	-0.41	-0.28
Standard deviation (°C)	0.21	0.26	0.20	0.23	0.30
$R^2$	0.98	0.97	0.99	0.99	0.95
RMSE (°C)	0.27	0.32	0.37	0.47	0.41

TABLE 6: Model fit between simulated and measured results for mean radiant temperature.

	Point 1	Point 2	Point 3	Point 4	Point 5
Minimum error (°C)	0	0.71	0.01	0.81	-0.07
Maximum error (°C)	-4.23	6.24	6.78	-6.25	-6.59
Mean error (°C)	0.08	1.10	0.88	-1.13	-0.6
Standard deviation (°C)	3.16	3.35	4.97	4.34	4.52
$R^2$	0.96	0.74	0.95	0.91	0.94
RMSE (°C)	3.16	3.56	5.05	4.49	4.56

Singapore [13], it can also be seen that the new ENVI-met model of version 4.0 shows much better performance than the previous version of ENVI-met 3.1. Since the thermal performance of different urban geometries and ground surface and their effect on mean radiant temperature can be modeled by ENVI-met, a relative comparison can be made for different design scenarios. In addition, the simulated results have been calibrated with field measurement data and then used as a benchmark for investigation of changes in design. Therefore, all the changes in design are consistent and relative to the simulated case, whereby the error from calibration has been effectively eliminated.

**3.2. Microclimate Differences.** It has been found from both the measurement and simulation results that the hottest time

is at 3 pm on the simulation day. Therefore, the effects of different landscape design scenarios on microclimate and thermal comfort are compared based on results at 3 pm. Except for the surface temperature, the other microclimate parameters are compared at 2.0 m above the ground level.

**3.2.1. Surface Temperature and Air Temperature.** Figure 6 shows the surface temperature patterns for all design scenarios. The differences in surface temperatures are obvious. Pavement with light-color granite (Scenario 2) has the lowest surface temperature, with a maximum reduction of 12°C compared with the base case. Surface temperature reduction by grass surfacing (Scenario 3) and adding more trees (Scenario 4) is also obvious, with a reduction by up to 8°C for grass and 10°C for trees.

Surface temperature reduction by applying wood pavement (Scenario 1) can be up to 6°C. Not much difference in surface temperature can be found by adding more water bodies. Both Scenario 6 (combination of light-color granite and adding more trees) and Scenario 7 (combination of grass surfacing and adding more trees) resulted in a significant reduction of surface temperature. However, Scenario 6 is more effective in reducing the surface temperature than Scenario 7.

Figure 7 shows the air temperature patterns for all design scenarios. The differences in air temperature between different scenarios are not so obvious as those in the surface temperature. The air temperature is about 0.25–0.75°C lower for the scenarios with light-color granite compared with the base case. For scenarios with grass surfacing and more trees, the air temperature reduction is about 0.25–0.5°C. For wood scenario, the apparent reduction of 6°C of the temperature at the surface does not cause a significant reduction in local air temperature at 2.0 m above the ground level. However, the air temperature of areas under building shade for the wood scenario is about 0.25°C lower than that in the base case. Scenario 6 and Scenario 7 both cause an air temperature reduction by up to 0.75°C.



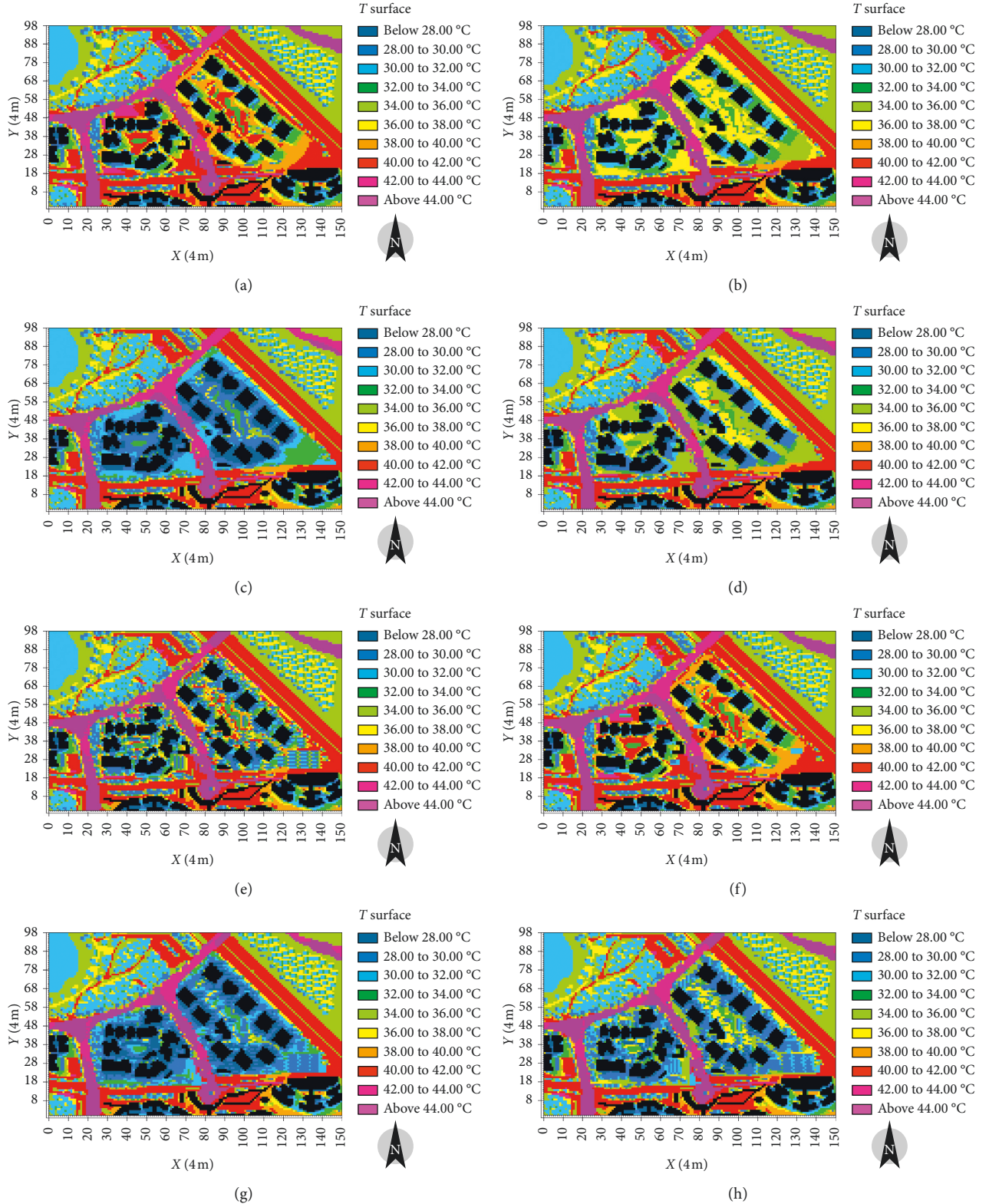


FIGURE 6: Simulated surface temperature for all design scenarios. (a) Base case. (b) Scenario 1 (wooden boards). (c) Scenario 2 (light-color granite). (d) Scenario 3 (grass surface). (e) Scenario 4 (more trees). (f) Scenario 5 (more water bodies). (g) Scenario 6 (light-color granite + more trees). (h) Scenario 7 (grass surface + more trees).

Not much difference in air temperature can be found for the scenario of adding more water bodies. Water bodies are found to be not effective in decreasing the air temperature in

Singapore in the current study. This is in agreement with a field measurement study conducted by Wong et al. [23] who investigated the evaporative cooling performance of

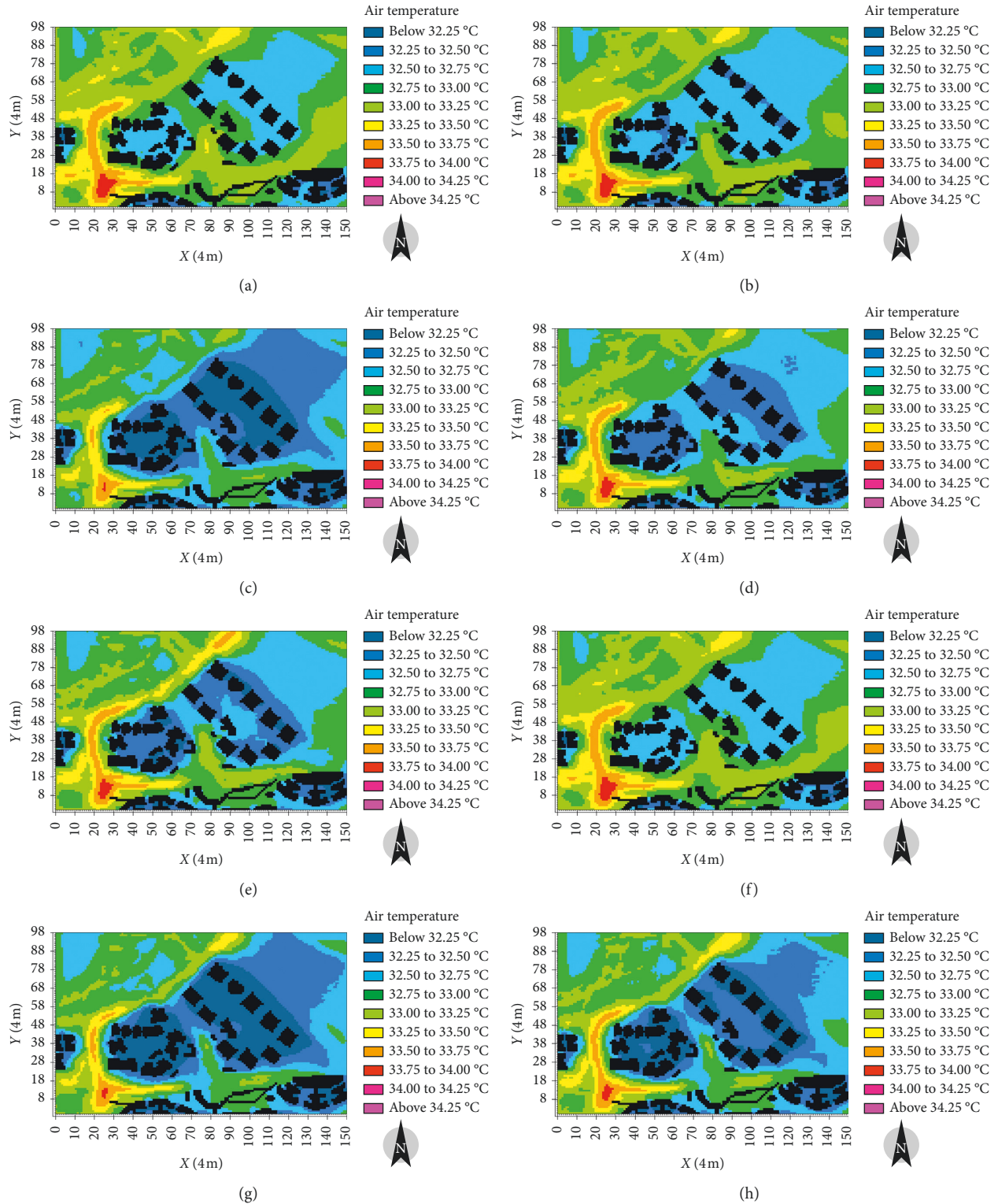


FIGURE 7: Simulated air temperature for all design scenarios. (a) Base case. (b) Scenario 1 (wooden boards). (c) Scenario 2 (light-color granite). (d) Scenario 3 (grass surface). (e) Scenario 4 (more trees). (f) Scenario 5 (more water bodies). (g) Scenario 6 (light-color granite + more trees). (h) Scenario 7 (grass surface + more trees).

a waterway in Singapore and found that the air temperature was merely reduced by 0.1°C on every 30 m away from the waterway. The high humidity climate and low wind condition might be one of the possible reasons for it.

**3.2.2. Mean Radiant Temperature.** The patterns of mean radiant temperature for all design scenarios are presented in Figure 8. For sunlit places, the mean radiant temperatures are 50–54°C for all scenarios except the grass surface



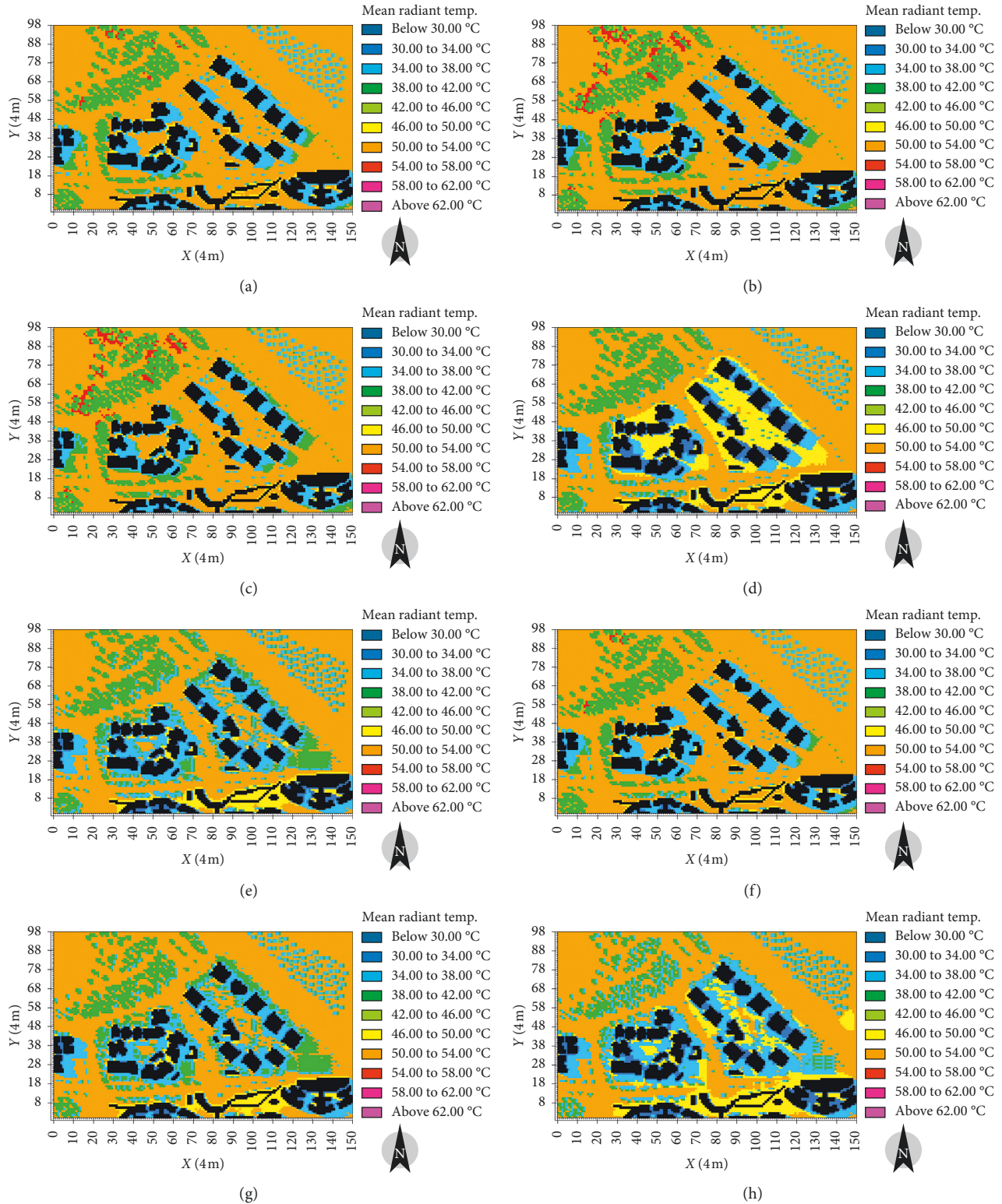


FIGURE 8: Simulated mean radiant temperature for all design scenarios. (a) Base case. (b) Scenario 1 (wooden boards). (c) Scenario 2 (light-color granite). (d) Scenario 3 (grass surface). (e) Scenario 4 (more trees). (f) Scenario 5 (more water bodies). (g) Scenario 6 (light-color granite + more trees). (h) Scenario 7 (grass surface + more trees).

scenarios, which have mean radiant temperatures 4–8°C lower than other scenarios. For places shaded by buildings, differences in mean radiant temperature are obvious. For

both the wood and light-color granite scenarios, the mean radiant temperatures are 4–8°C higher than those of the base case. For the tree scenarios, there is a significant cooling

effect and the mean radiant temperature under tree-shaded areas can be reduced by 12–16°C compared with sunlit areas. Scenario 7 (combination of grass surface and more trees) is the best with 4–8°C mean radiant temperature reduction for areas exposed to the sun and 12–16°C reduction for tree-shaded areas. Not much difference can be found for the scenario of adding more water bodies.

The results from ENVI-met indicate that the change of pavement materials has a minor effect on reducing mean radiant temperature for places exposed to high solar radiation. For places shaded by buildings, the mean radiant temperature is even increased by using high-albedo pavement materials. This is consistent with other studies which also found increases of mean radiant temperature by applying high-albedo materials [4, 16, 24] in hot and humid climates.

**3.2.3. Wind Speed and Relative Humidity.** Due to the small differences between different design scenarios in terms of wind speed and relative humidity, the figures are not shown here. The results show that wind speed is slightly reduced by 0.2 m/s with more trees planting. The differences in wind speed are not obvious for other design scenarios. This is because the layout of building blocks has been determined in the residential quarters for this study. Compared with landscape elements, the layout of building blocks has greater effect on air flow in urban spaces.

As to the relative humidity, scenarios with grass surface, more trees, and water bodies are more humid, with an increase of 4% to 6% compared with the base case. The change of landscape elements cannot lead to significant variation of relative humidity when the humidity is very high throughout the year. This is the climate in Singapore, and hence, the results make sense.

**3.3. Thermal Comfort Maps of PET.** Figure 9 shows the simulated thermal comfort (PET) maps for all the design scenarios at 3 pm. The PET values of sunlit places for all the design scenarios are dominated by extremely hot condition with the PET between 46 and 50°C, which is under severe heat stress and far above the comfortable temperature range (24–30°C) required for Singapore occupants (Table 4). Although thermal comfort is difficult to achieve under such hot climate conditions, some improvements can be made through landscape design.

The best thermal conditions are in the areas with shading, either shaded by buildings or trees, with a PET of 34–38°C, which corresponds to “warm” according to Table 4. The shade enhancement by trees or buildings has a clear positive effect on alleviating outdoor heat stress, as indicated by decreased PET.

Scenario 3 (grass surface) only leads to a PET reduction of 4–8°C for limited areas, and the heat stress conditions for most of the study areas are not improved. Scenarios with trees (4, 6, and 7) have the same PET patterns despite that each

scenario has different pavement materials. Again adding more water bodies is found to have little effect on PET.

## 4. Discussion

Table 7 summarizes the effect of different design scenarios on microclimate and human thermal comfort (PET).

It can be seen that design strategies that can reduce surface temperature and air temperature may not necessarily reduce heat stress condition. Design strategies such as applying wooden boards and light-color granite have some extent of cooling effect, but heat stress is marginally reduced. Both the wooden board and light-color granite are high-albedo materials with an albedo of 0.8 in this study. While higher albedo reduces the surface temperatures, and consequently, the air temperature, it increases the amount of reflected short-wave radiation in the environment at the same time. As it is known, the increase of energy flux will result in the increase of mean radiant temperature. Mean radiant temperature is the main factor affecting outdoor thermal comfort in hot and humid climate as in Singapore [17]. Thus, the insignificant effect of high-albedo materials on reducing heat stress can be expected. However, the effectiveness of high-albedo covering on heat stress is disputed because PET does not take surface temperature into consideration. The decrease of surface temperature is not reflected in PET, which raises a question of whether surface temperature has an effect on urban thermal comfort. Different from the indoor environment which has uniform and relative lower surface temperatures, outdoor space has a large variation and fluctuation of surface temperatures. The evaluation of urban thermal comfort is a challenging topic in the research field of human bioclimate, which still needs further study.

Water can mitigate the urban heat island effect since more incoming heat can be transformed into latent heat rather than sensible heat. However, water bodies are found to be not effective in mitigating heat stress in hot and humid climate as studied in this paper. Adding more water bodies does not change any microclimate parameters except that humidity increases slightly. This may be because the area of water bodies in this study is not large enough to create a cooling effect for the surrounding environment. Besides, due to the high humidity conditions in Singapore, thermal comfort cannot benefit too much from the evaporation from water bodies.

It has been widely accepted that shading is the key strategy for promoting outdoor thermal comfort in hot climate. Interception of solar radiation is the most effective means in improving thermal comfort in outdoor areas in hot and dry climate [6]. The current study also vindicates this design principle because the scenarios shaded by more trees have the best thermal comfort condition, with the maximum PET reduced by 12°C. However, not much difference is found for scenarios with trees (Scenario 4, 6, and 7) in terms of urban heat stress even though each scenario has different pavement materials. Different pavement materials can lead to variations in surface temperature, air temperature, and mean radiant temperature in urban spaces, but these

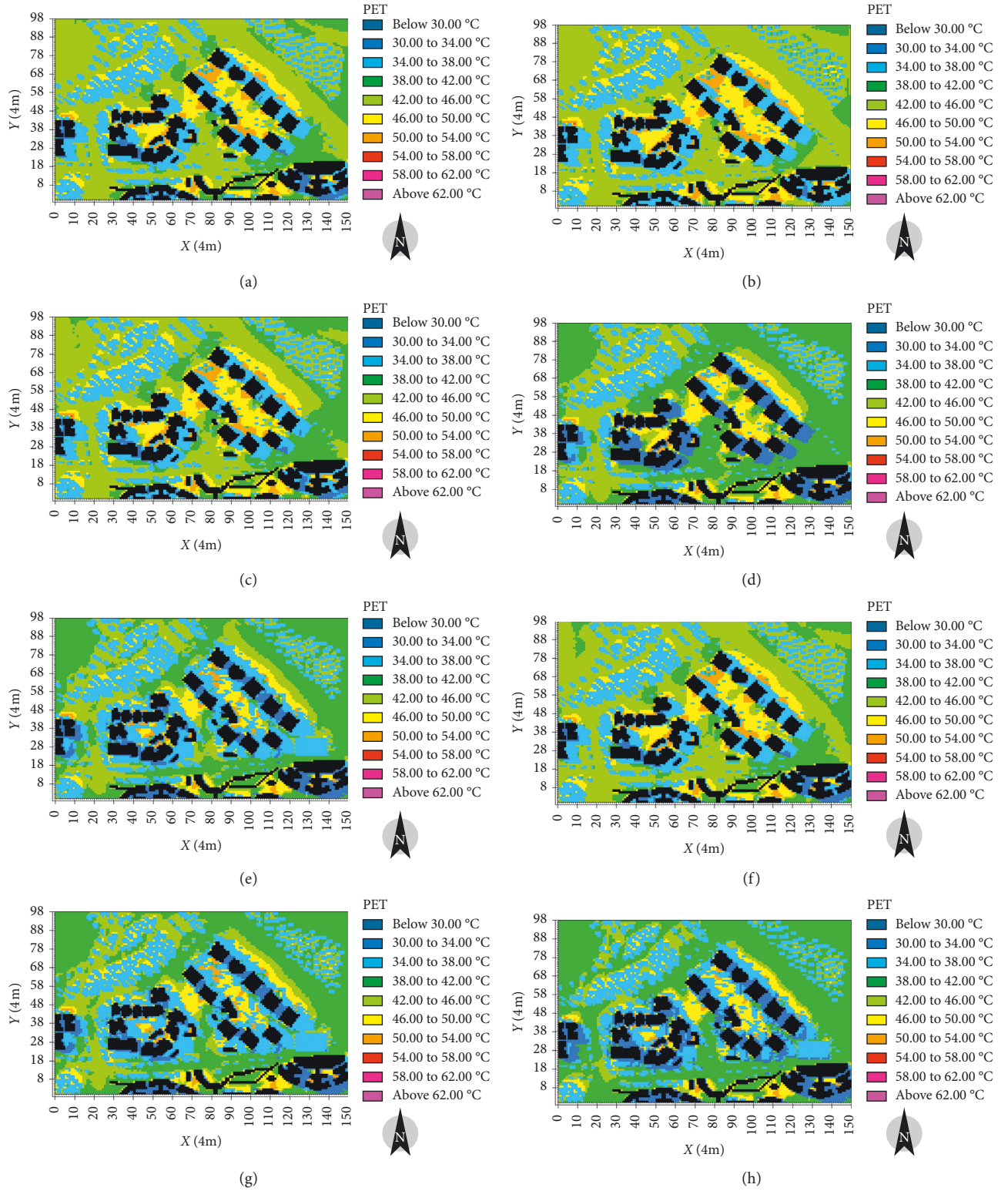


FIGURE 9: Simulated PET for all the design scenarios. (a) Base case. (b) Scenario 1 (wooden boards). (c) Scenario 2 (light-color granite). (d) Scenario 3 (grass surface). (e) Scenario 4 (more trees). (f) Scenario 5 (more water bodies). (g) Scenario 6 (light-color granite + more trees). (h) Scenario 7 (grass surface + more trees).



TABLE 7: Summary of the effect of different design scenarios on urban microclimate and thermal comfort (PET).

Design scenarios		Surface temp. reduction	Air temp. reduction	Mean radiant temp. reduction	PET reduction
1	Wooden boards	2–6°C	0–0.25°C for building-shaded areas	–8 to –4°C for building-shaded areas	No change
2	Light-color granite	2–12°C		–8 to –4°C for building-shaded areas	No change
3	Grass surface	2–8°C	0.25–0.5°C	4–8°C for areas exposed to the sun	4–8°C for limited areas
4	More trees	2–10°C	0.25–0.5°C	12–16°C for tree-shaded areas	4–12°C
5	More water bodies	No change	No change	No change	No change
6	Light-color granite and more trees	2–12°C	0.25–0.75°C	–8 to –4°C for building-shaded areas 12–16°C for tree-shaded areas	4–12°C
7	Grass surface and more trees	2–10°C	0.25–0.75°C	4–8°C for areas exposed to the sun 12–16°C for tree-shaded areas	4–12°C

variations may not be effective enough to reduce heat stress during the daytime. However, during the night, the effect of different pavement materials on thermal comfort can be obvious because different materials have different thermal properties. In addition, air temperature is the main factor that affects urban thermal comfort during the nighttime. It needs to be noted that due to time constraints and limitations of ENVI-met modeling, nighttime thermal comfort is not investigated in this study.

Compared with grass surfacing, tree planting is a more effective strategy to promote shading, thus reducing urban heat stress. Although tree planting would lead to an increase of relative humidity and a decrease of wind speed, those negative effects are minor compared with the positive effects of reduction of air temperature and mean radiant temperature. As predicted, the combination of shade trees over grass is found to be the most effective landscape strategy in terms of cooling provided, with the maximum surface temperature reduced by 10°C, air temperature reduced by 0.75°C, mean radiant temperature reduced by 16°C, and PET reduced by 12°C.

## 5. Conclusions

The effects of urban landscape design on urban microclimate and thermal comfort in a high-rise residential area in the tropic climate of Singapore have been investigated in this paper. Various landscape elements of pavement materials, greenery, and water bodies have been studied. Real data on microclimate obtained from a comprehensive field measurement with multiple points have been presented and used to calibrate the new version of the microclimate-modeling software EVNI-met. With the calibrated ENVI-met, seven urban design scenarios of different surface albedo, greenery, and water bodies have been simulated with different microclimatic parameters, and their effects on human thermal comfort as measured by PET have been evaluated. It has been found that the maximum improvement of PET between the existing landscape (i.e., the base case) and suggested landscape design is about 12°C, and achieving thermal comfort during the hottest time of the day is impossible. It has also been found that the combination of shade trees over grass is the most effective landscape strategy for cooling with

the maximum surface temperature reduced by 10°C, air temperature reduced by 0.75°C, mean radiant temperature reduced by 16°C, and PET reduced by 12°C. Although high-albedo pavement materials and water bodies are found not effective in reducing heat stress in hot and humid climate conditions, the results are dubious since the evaluation of urban thermal comfort does not include the surface temperature. The evaluation of urban thermal comfort is a challenging topic in the research field of human bioclimate, which still needs further study. It can be concluded that the findings from the paper can equip urban planners and designers with knowledge and techniques when they plan for future urban areas/regions and replan for existing urban areas/regions so as to mitigate urban heat stress. However, due to the limitations of ENVI-met modeling, the effect of landscape design on nighttime thermal comfort and urban heat island requires further investigation in the future.

## Data Availability

The data used to support the findings of this study are available from the corresponding author upon request.

## Conflicts of Interest

The authors declare that they have no conflicts of interest.

## Acknowledgments

This work was supported by the NUS Research Scholarship from the National University of Singapore and Natural Science Foundation of Hubei Province, China, under Grant number 2015CFB510. The authors would like to express their sincere thanks to Professor Wong Nuyk Hien and his Ph.D. students from the National University of Singapore for their assistance in the field measurement work of this paper.

## References

- [1] F. Salata, I. Golasi, R. de Lieto Vollaro, and A. de Lieto Vollaro, "Urban microclimate and outdoor thermal comfort. A proper procedure to fit ENVI-met simulation outputs to experimental data," *Sustainable Cities and Society*, vol. 26, pp. 318–343, 2016.

- [2] M. W. Yahia, E. Johansson, S. Thorsson, F. Lindberg, and M. I. Rasmussen, "Effect of urban design on microclimate and thermal comfort outdoors in warm-humid Dar es Salaam, Tanzania," *International Journal of Biometeorology*, vol. 62, no. 3, pp. 373–385, 2018.
- [3] F. Ali-Toudert and H. Mayer, "Effects of asymmetry, galleries, overhanging facades and vegetation on thermal comfort in urban street canyons," *Solar Energy*, vol. 81, no. 6, pp. 742–754, 2007.
- [4] R. Emmanuel, H. Rosenlund, and E. Johansson, "Urban shading—a design option for the tropics? A study in Colombo, Sri Lanka," *International Journal of Climatology*, vol. 27, no. 14, pp. 1995–2004, 2007.
- [5] E. Ng, L. Chen, Y. Wang, and C. Yuan, "A study on the cooling effects of greening in a high-density city: an experience from Hong Kong," *Building and Environment*, vol. 47, pp. 256–271, 2012.
- [6] N. Mazhar, R. D. Brown, N. Kenny, and S. Lenzholzer, "Thermal comfort of outdoor spaces in Lahore, Pakistan: lessons for bioclimatic urban design in the context of global climate change," *Landscape and Urban Planning*, vol. 138, pp. 110–117, 2015.
- [7] A. M. Hunter, N. S. G. Williams, J. P. Rayner, L. Aye, D. Hes, and S. J. Livesley, "Quantifying the thermal performance of green facades: a critical review," *Ecological Engineering*, vol. 63, pp. 102–113, 2014.
- [8] R. D. Brown and T. J. Gillespie, "Estimating outdoor thermal comfort using a cylindrical radiation thermometer and an energy budget model," *International Journal of Biometeorology*, vol. 30, no. 1, pp. 43–52, 1986.
- [9] R. D. Brown, "Ameliorating the effects of climate change: modifying micro-climates through design," *Landscape and Urban Planning*, vol. 100, no. 4, pp. 372–374, 2011.
- [10] M. W. Yahia and E. Johansson, "Landscape interventions in improving thermal comfort in the hot dry city of Damascus, Syria—the example of residential spaces with detached buildings," *Landscape and Urban Planning*, vol. 125, pp. 1–16, 2014.
- [11] K. Perini and A. Magliocco, "Effects of vegetation, urban density, building height, and atmospheric conditions on local temperatures and thermal comfort," *Urban Forestry and Urban Greening*, vol. 13, no. 3, pp. 495–506, 2014.
- [12] H. Lee, H. Mayer, and L. Chen, "Contribution of trees and grasslands to the mitigation of human heat stress in a residential district of Freiburg, Southwest Germany," *Landscape and Urban Planning*, vol. 148, pp. 37–50, 2016.
- [13] W. Yang, N. H. Wong, and C. Q. Li, "Effect of street design on outdoor thermal comfort in an urban street in Singapore," *Journal of Urban Planning and Development*, vol. 142, no. 1, article 05015003, 2016.
- [14] M. Bruse and H. Fleer, "Simulating surface-plant-air interactions inside urban environments with a three dimensional numerical model," *Environmental Modelling and Software*, vol. 13, no. 3–4, pp. 373–384, 1998.
- [15] *ENVI-met 4.0 (Computer Software)*, Michael Bruse & Team, Bochum, Germany, <http://www.envi-met.com/>.
- [16] F. Yang, S. S. Y. Lau, and F. Qian, "Thermal comfort effects of urban design strategies in high-rise urban environments in a sub-tropical climate," *Architecture Science Review*, vol. 54, no. 4, pp. 285–304, 2011.
- [17] W. Yang, N. H. Wong, and G. Zhang, "A comparative analysis of human thermal conditions in outdoor urban spaces in summer season in Singapore and Changsha, China," *International Journal of Biometeorology*, vol. 57, no. 6, pp. 895–907, 2013.
- [18] A. Matzarakis, F. Rutz, and H. Mayer, "Modeling radiation fluxes in simple and complex environments—application of the RayMan model," *International Journal of Biometeorology*, vol. 51, no. 4, pp. 323–334, 2007.
- [19] A. Matzarakis, F. Rutz, and H. Mayer, "Modeling radiation fluxes in simple and complex environments: basics of the RayMan model," *International Journal of Biometeorology*, vol. 54, no. 2, pp. 131–139, 2010.
- [20] A. N. Kakon, N. Mishima, and S. Kojima, "Simulation of the urban thermal comfort in a high density tropical city: analysis of the proposed urban construction rules for Dhaka, Bangladesh," *Building Simulation*, vol. 2, no. 4, pp. 291–305, 2009.
- [21] C. Ketterer and A. Matzaraki, "Comparison of different methods for the assessment of the urban heat island in Stuttgart, Germany," *International Journal of Biometeorology*, vol. 59, no. 9, pp. 1299–1309, 2015.
- [22] E. L. Krüger, F. O. Minella, and F. Rasia, "Impact of urban geometry on outdoor thermal comfort and air quality from field measurements in Curitiba, Brazil," *Building and Environment*, vol. 46, no. 3, pp. 621–634, 2011.
- [23] N. H. Wong, C. Tan, A. Nindyani, S. Jusuf, and E. Tan, "Influence of water bodies on outdoor air temperature in hot and humid climate," in *Proceedings of International Conference on Sustainable Design and Construction (ICSDC 2011)*, Kansas City, MO, USA, March 2011.
- [24] F. Salata, I. Golasi, A. de Lieto Vollaro, and R. de Lieto Vollaro, "How high albedo and traditional buildings' materials and vegetation affect the quality of urban microclimate. A case study," *Energy and Buildings*, vol. 99, pp. 32–49, 2015.



